

Linear stability analysis of Taylor-Couette flow in a viscoelastic fluid under out-of phase modulation

M. Riahi¹, S. Aniss¹, M. T. Ouazzani¹, and S. Skali Lami²

¹University of Hassan II, Faculty of Sciences Aïn-Chock,
Laboratory of Mechanics, B.P.5366 Mâarif, Casablanca, Morocco

²University of Lorraine, Lemta-UMR CNRS 7563-Ensem, 2 avenue de la Forêt de Haye, BP 160,
Vandoeuvre les Nancy, 54504, France

Copyright © 2014 ISSR Journals. This is an open access article distributed under the **Creative Commons Attribution License**, which permits unrestricted use, distribution, and reproduction in any medium, provided the original work is properly cited.

ABSTRACT: In this work, the linear stability analysis of a pulsed Taylor-Couette flow is investigated in the case of a linear Maxwell fluid when both cylinders are subjected to an out-of phase modulation with equal modulation amplitude and equal modulation frequency. The linear problem is solved using the Floquet theory and a technique of converting a boundary value problem to an initial value problem. Attention is focused on the influence of elasticity on the critical parameters corresponding to the onset of instability. The numerical results show that the Deborah number has a destabilizing effect in the high frequency limit and the critical parameters are independent on the frequency number. However, in the low frequency limit the Maxwell fluid behaves as a Newtonian one and no effect of Deborah number is observed.

KEYWORDS: Linear stability; Pulsed Taylor-Couette flow; Maxwell fluid; Floquet theory.

1 INTRODUCTION

Several studies devoted to the modulation of the Taylor-Couette flow have been conducted both experimentally and theoretically in different configurations in which the angular velocities of the inner and outer cylinders are respectively, $\Omega_1 + \varepsilon_1 \cos(\omega t^*)$ and $\Omega_2 + \varepsilon_2 \cos(\omega t^*)$. The effect of the modulation on the threshold of instability compared to the unmodulated case was discussed in [1-2-3-4-5-6-7-8-9]. Otherwise, two configurations corresponding to a zero mean modulation, $\Omega_1 = \Omega_2 = 0$, in phase $\varepsilon_1 = \varepsilon_2 = 1$ or out of phase $\varepsilon_1 = -\varepsilon_2$ have been revisited theoretically in the narrow gap approximation in [10-11-12] and the first experimental evidence of these configurations was achieved in these investigations. The experimental results, corresponding to the modulation in phase, have been in good agreement with the linear stability analysis and both experimental and theoretical results have showed that the flow is less unstable in the limit of low and high frequency while destabilization is maximum for an intermediate frequency. For modulation in out of phase, the numerical results in [12] compared well with the experimental observations at high and moderate frequencies but showed a disagreement at low frequencies.

In contrast to these works which have examined the case of a Newtonian fluid, we perform in this paper a linear stability analysis of the pulsed Taylor-Couette flow in a viscoelastic fluid which is modeled by a linear Maxwell model. Considering the narrow gap approximation, we investigate in the case of an out-of phase zero mean modulation, the effect of frequency modulation and elasticity characterized by Deborah number on the threshold of instability.

2 MATHEMATICAL FORMULATION

Consider the time periodic flow in an incompressible viscoelastic fluid filling the annulus space between two infinitely long cylinders of radii R_1 and $R_2 = R_1 + d$ with d being the gap width, Fig. 1. The angular velocity of the inner and the outer

cylinders are respectively $\Omega_1 = \Omega_0 \cos(\omega t^*)$ and $\Omega_2 = -\Omega_0 \cos(\omega t^*)$. The quantities Ω_0 and ω denote respectively the amplitude and the adimensional frequency of the modulated rotation.

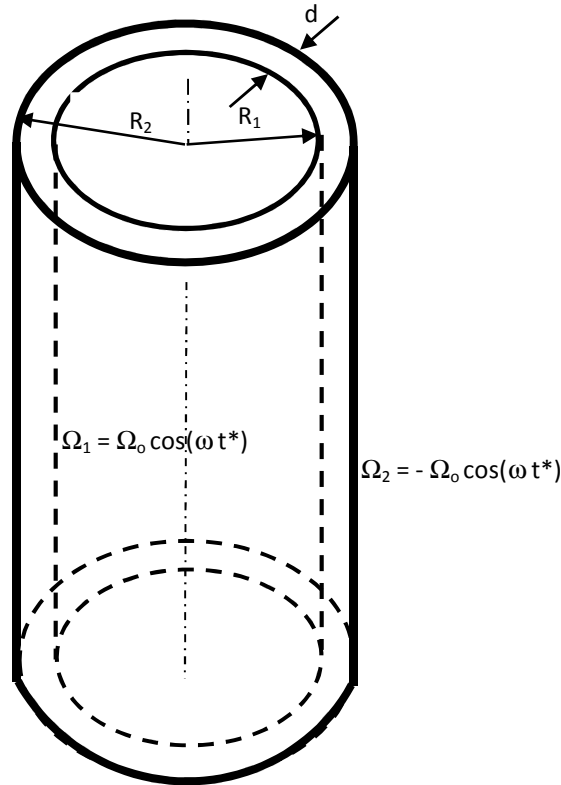


Fig 1. Viscoelastic fluid confined in a Taylor-Couette system with rotation modulation of the inner and outer cylinders

The governing equations are the momentum and mass equations which are given by

$$\frac{\partial \mathbf{V}^*}{\partial t^*} + \mathbf{V}^* \cdot \nabla \mathbf{V}^* = -\frac{1}{\rho} \nabla P^* + \nu \nabla \cdot \boldsymbol{\tau} \tag{1}$$

$$\nabla \cdot \mathbf{V}^* = 0 \tag{2}$$

where \mathbf{V}^* is the velocity vector, $\boldsymbol{\tau}$ is the extra stress tensor, P^* is the pressure and ν is the kinematic viscosity. The fluid is assumed to obey a linear Maxwell model and can be represented by a purely viscous damper and a purely elastic spring connected in series

$$\boldsymbol{\tau} + \lambda \frac{\partial}{\partial t^*} \boldsymbol{\tau} = \mu \mathbf{ID} \tag{3}$$

We denote by \mathbf{ID} the rate of strain tensor defined by $\mathbf{ID} = \nabla \mathbf{V}^* + \nabla^t \mathbf{V}^*$ and we designate by ρ the density, μ the dynamic viscosity and λ the relaxation time.

2.1 BASE FLOW

In dimensional cylindrical-polar coordinates (r^*, θ, z^*) , the velocity components are denoted respectively, in the radial, azimuthal and axial direction, by (U^*, V^*, W^*) . Hereafter, we assume that the base flow is azimuthal and axisymmetric and then it is written as $\mathbf{V}^* = (0, V^*, 0)$ with P^* and V^* are θ independents. Under these assumptions, a combination of the equations (1 – 2 – 3) leads to the following system

$$\rho \left(1 + \lambda \frac{\partial}{\partial t^*}\right) \left(-\frac{V^{*2}}{r^*}\right) = -\left(1 + \lambda \frac{\partial}{\partial t^*}\right) \left(\frac{\partial P^*}{\partial r^*}\right) \tag{4}$$

$$\rho \left(1 + \lambda \frac{\partial}{\partial t^*}\right) \frac{\partial V^*}{\partial t^*} = \mu \left(\frac{\partial^2 V^*}{\partial r^{*2}} + \frac{\partial}{\partial r^*} \left(\frac{V^*}{r^*}\right)\right) \tag{5}$$

$$0 = -\left(1 + \lambda \frac{\partial}{\partial t^*}\right) \left(\frac{\partial P^*}{\partial z^*}\right) \tag{6}$$

We introduce the following dimensionless variables

$$r^* = R_1 + d x, \quad t = \frac{t^*}{\frac{d^2}{\nu}}, \quad V_B = \frac{V^*}{R_1 \Omega_0}, \quad P_B = \frac{P^*}{\rho R_1 d \Omega_0^2}$$

Equation (6) shows that the pressure is independent of z^* . Assuming that the gap width d is small compared to the radius R_1 of the inner cylinder and using the small-gap approximation in which all terms of order d/R_1 are neglected, the dimensionless azimuthal velocity of the basic state satisfies equation (5) which is now in the form

$$\Gamma \frac{\partial^2 V_B}{\partial t^2} + \frac{\partial V_B}{\partial t} = \frac{\partial^2 V_B}{\partial x^2} \tag{7}$$

with the boundary conditions

$$V_B(x = 0, t) = \cos(\sigma t), \quad V_B(x = 1, t) = -\cos(\sigma t) \tag{8}$$

The parameters $\sigma = \omega d^2/\nu$ and $\Gamma = \lambda \nu/d^2$ are respectively the frequency number and Deborah number. The parameter σ is the ratio of the viscous diffusive time and the period of modulation whereas Γ is the ratio of the relaxation time and viscous diffusive time. The pressure of the base flow, P_B , is obtained from equation (4) which is written as

$$\rho \left(1 + \Gamma \frac{\partial}{\partial t^*}\right) V_B = - \left(1 + \Gamma \frac{\partial}{\partial t^*}\right) \left(\frac{\partial P_B}{\partial x}\right)$$

The solution of Equations (7) and (8) is of the form

$$V_B(x, t) = V_1(x) \cos(\sigma t) + V_2(x, t) \sin(\sigma t) \tag{9}$$

The functions V_1 and V_2 are given by

$$V_1(x) = \frac{\cos(\gamma \beta x) \cosh(\gamma \xi (1-x)) - \cos(\gamma \beta (1-x)) \cosh(\gamma \xi x)}{\cosh(\gamma \xi) - \cos(\gamma \beta)}$$

$$V_2(x) = \frac{\sin(\gamma \beta x) \sinh(\gamma \xi (1-x)) - \sin(\gamma \beta (1-x)) \sinh(\gamma \xi x)}{\cosh(\gamma \xi) - \cos(\gamma \beta)}$$

where $\gamma = \sqrt{\frac{\sigma}{2}}$, $\beta = \sqrt{\sigma\Gamma + \sqrt{1 + \Gamma^2\sigma^2}}$, $\xi = \sqrt{\sigma\Gamma - \sqrt{1 + \Gamma^2\sigma^2}}$. The parameter γ expresses the ratio of two lengths $\gamma = d/\delta_N$ where $\delta_N = \sqrt{2\nu/\omega}$ is the thickness of the Stokes layer for a Newtonian fluid. The parameters β and ξ express also the ratio of two lengths, indeed $\beta = \xi^{-1} = \delta_M/\delta_N$ where $\delta_M = d (\sigma/2)^{-1/2} (\sigma\Gamma + \sqrt{1 + \sigma^2\Gamma^2})^{-1/2}$ is the thickness of the Stokes layer for a linear Maxwell fluid defined in [13].

2.2 LINEAR STABILITY AND NUMERICAL APPROACH

The linear stability of the base flow respecting axisymmetric disturbances is considered. The velocity and the pressure fields in the perturbed state are written as the sum of the base flow variables and small perturbations

$$\mathbf{u} = (0, V_B, 0) + (u(x, z, t), v(x, z, t), w(x, z, t)) \tag{10}$$

$$P = P_B + p(x, z, t) \tag{11}$$

Substituting expressions (10) and (11) into equations (4)-(5) and linearizing yields

$$\left(M - \frac{\partial}{\partial t} - \Gamma \frac{\partial^2}{\partial t^2}\right) u + 2 T_a^2 V_B v = \left(1 + \Gamma \frac{\partial}{\partial t}\right) \left(\frac{\partial p}{\partial x}\right) \tag{12}$$

$$\left(M - \frac{\partial}{\partial t} - \Gamma \frac{\partial^2}{\partial t^2}\right) v = \left(1 + \Gamma \frac{\partial}{\partial t}\right) \left(\frac{\partial V_B}{\partial x}\right) u \tag{13}$$

$$\left(M - \frac{\partial}{\partial t} - \Gamma \frac{\partial^2}{\partial t^2}\right) w = \left(1 + \Gamma \frac{\partial}{\partial t}\right) \left(\frac{\partial p}{\partial z}\right) \tag{14}$$

$$\frac{\partial u}{\partial x} + \frac{\partial w}{\partial x} = 0 \quad (15)$$

The boundary conditions for perturbations are

$$u = v = w = 0 \text{ at } x = 0,1 \quad (16)$$

where $M = \frac{\partial^2}{\partial x^2} + \frac{\partial^2}{\partial z^2}$ and T_a is the Taylor number defined as $Ta = (R_1 \Omega_0 d / \nu) \sqrt{d/R_1}$. Hereafter, we seek the solution of the system of equations (12--15) in terms of normal modes as

$$(u, v, w, p) = (\tilde{u}(x, t), \tilde{v}(x, t), \tilde{w}(x, t), \tilde{p}(x, t)) \exp(iqz) \quad (17)$$

where q is the axial wave number and i verifies $i^2 = -1$. Eliminating the pressure and the third component of velocity, the linearized equations governing the behavior of the eigenfunctions $\tilde{u}(x, t)$ and $\tilde{v}(x, t)$ become

$$\left(\Delta - \frac{\partial}{\partial t} - \Gamma \frac{\partial^2}{\partial t^2}\right) \Delta \tilde{u} = 2q^2 T_a^2 \left(1 + \Gamma \frac{\partial}{\partial t}\right) V_B \tilde{v} \quad (18)$$

$$\left(\Delta - \frac{\partial}{\partial t} - \Gamma \frac{\partial^2}{\partial t^2}\right) \tilde{v} = \left(1 + \Gamma \frac{\partial}{\partial t}\right) \left(\frac{\partial V_B}{\partial x}\right) \tilde{u} \quad (19)$$

where $\Delta = \frac{\partial^2}{\partial x^2} - q^2$. The boundary conditions of the system (18) – (19) are

$$\tilde{u} = \tilde{v} = \frac{\partial \tilde{u}}{\partial x} = 0 \text{ at } x = 0,1 \quad (20)$$

The numerical approach used in this work was employed in the studies related to the instability of modulated flows [10-11-12-14]. The system of equations (18) and (19) is solved using the Floquet theory and then, the perturbed quantities are expanded in the form

$$(\tilde{u}, \tilde{v}) = \exp(\mu t) \sum_{n=-\infty}^{n=+\infty} (U_p(x), V_p(x)) \exp(in\sigma t) \quad (21)$$

The Floquet exponent $\mu = \mu_0 + i\mu_1$ is a complex number. Here, we aim to determine the marginal stability corresponding to harmonic solutions *i.e.* $\mu_0 = \mu_1 = 0$. Hereafter, the base flow is rewritten as

$$V_B = F(x) \exp(i\sigma t) + F^*(x) \exp(-i\sigma t) \quad (22)$$

where $F(x) = \frac{1}{2}(V_1(x) - iV_2(x))$ and the starred quantity means the complex conjugate. Introducing expressions (21) and (22) into the system (18)-(19), we obtain an infinite set of equations

$$(D^2 - q^2 - in\sigma + \Gamma n^2 \sigma^2)(D^2 - q^2)U_n = 2q^2 T_a^2 (1 + i\Gamma n\sigma)(FV_{n-1} + F^*V_{n+1}) \quad (23)$$

$$(D^2 - q^2 - in\sigma + \Gamma n^2 \sigma^2)V_n = (1 + i\Gamma n\sigma) \left(\frac{dF}{dx} U_{n-1} + \frac{dF^*}{dx} U_{n+1}\right) \quad (24)$$

where $D = \frac{d}{dx}$ and the associated boundary conditions are

$$u_n = v_n = Du_n = 0 \text{ at } x = 0,1 \quad (25)$$

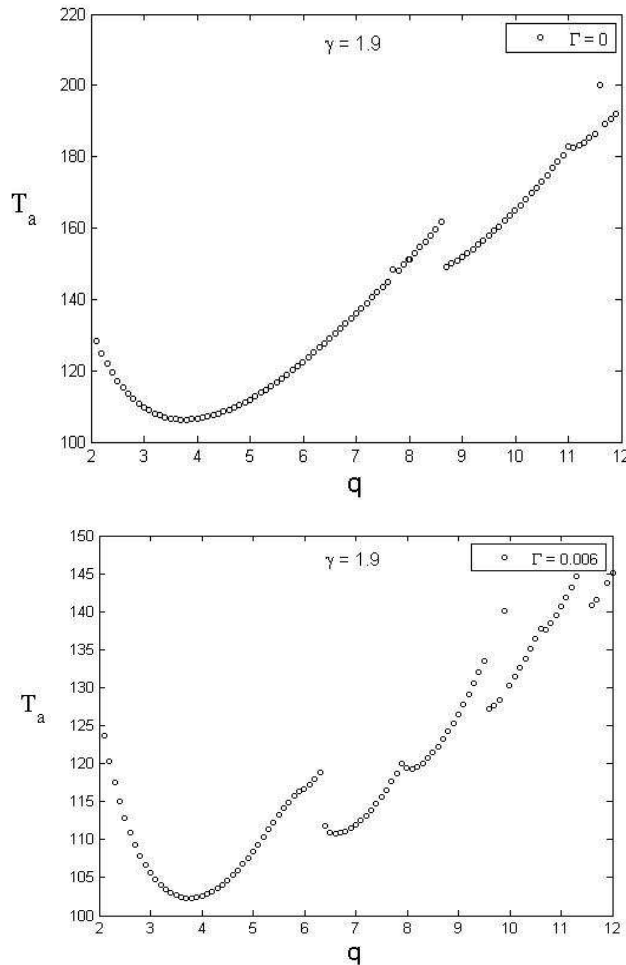
The system (23)-(24) is transformed into a set of first-order ordinary differential equations for the quantities, $U_n, DU_n, (D^2 - q^2)U_n, D(D^2 - q^2)U_n, V_n$ and DV_n . A set of $3 + 6N$ independent solutions satisfying the boundary conditions (25) at $x = 0$ is constructed by a Runge-Kutta numerical scheme [14]. A linear combination of these solutions satisfying the boundary conditions (25) at the other extreme $x = 1$ leads to a homogeneous algebraic system for the coefficients of the combination. A necessary condition for the existence of nontrivial solution is the vanishing of the determinant which can be formally written as

$$F(\sigma, q, T_a, \Gamma) = 0$$

For assigned values of the frequency number, σ , and Deborah number, Γ , the neutral curves $T_a(q)$ are obtained and then the critical Taylor and wave numbers, T_{ac} and q_c , are determined. The convergence of the numerical solutions depends greatly on the order N of the truncated Fourier series where $-N \leq n \leq N$. The number of modes N retained in the system (23)-(24) depends strongly on the frequency value. For instance, $N = 3$ and $N = 11$ are the orders of the Fourier series for high and low frequency respectively.

3 NUMERICAL RESULTS AND DISCUSSION

We investigate the effect of Deborah number on the onset of instability in a linear Maxwell fluid confined between two out-of-phase oscillating cylinders with the same amplitudes and frequency. Thereafter, this effect is analyzed by determining the critical parameters, Taylor and wave numbers, versus the parameter $\gamma = \sqrt{\frac{\sigma}{2}}$ in which σ is the dimensionless frequency of modulation. For instance, we show in Fig.2 the marginal stability curves when $\gamma = 1.9$ for different values of Deborah number. As one can see, the shape of these curves is affected by Deborah number and the number of minimums increases with this number. Also, one can note that the smaller value of these minimums corresponding to the critical Taylor number decreases when Deborah number weakly increases. This first observation confirms the destabilizing effect of Deborah number.



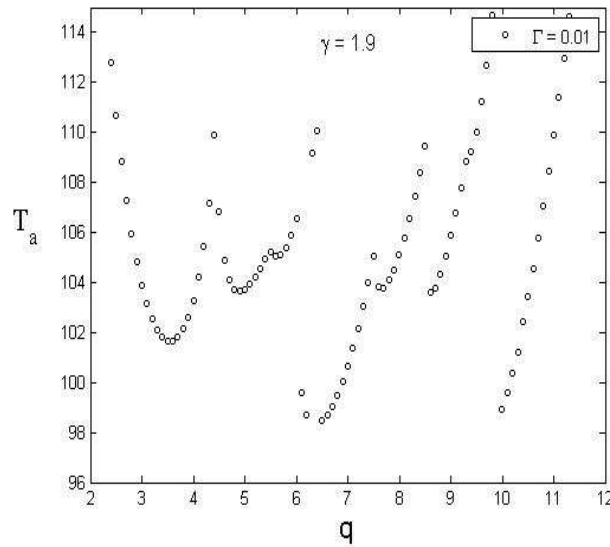


Fig. 2. Marginal stability curves for $\gamma = \sqrt{\frac{\sigma}{2}} = 1.9$ and for different values of Deborah number Γ .

The critical Taylor number versus the parameter γ is reported in Fig. 3 for different values of Deborah number. The numerical results in the case of a Newtonian fluid, $\Gamma = 0$, are compared to the numerical and experimental ones obtained in [5] and [11] and show an excellent agreement. As observed in Fig. 3, a change in the shape of the curves is revealed in the high frequency limit. Indeed, in contrast to the Newtonian fluid case, $\Gamma = 0$, where the critical Taylor number increases with the frequency number γ , we note that at $\Gamma = 0.001$, $\Gamma = 0.006$ and $\Gamma = 0.008$, the critical Taylor number varies independently on the frequency number and tends respectively to the values : $T_{ac} = 863.32$, $T_{ac} = 223.03$ and $T_{ac} = 198.25$. Furthermore, in the high frequency limit, the increase of Deborah number leads to a destabilization of the base flow. This destabilizing effect is observed for $\gamma > 1$ and becomes more pronounced as the frequency number increases. However, when the frequency number tends to zero, *i.e.* long period of modulation, the critical Taylor number reproduces quite well the classical Taylor-Couette solution corresponding to the steady rotation of the cylinders for a Newtonian fluid, $T_{ac} = 68.91$. In this frequency limit, the Deborah number has no effect on the critical Taylor number.

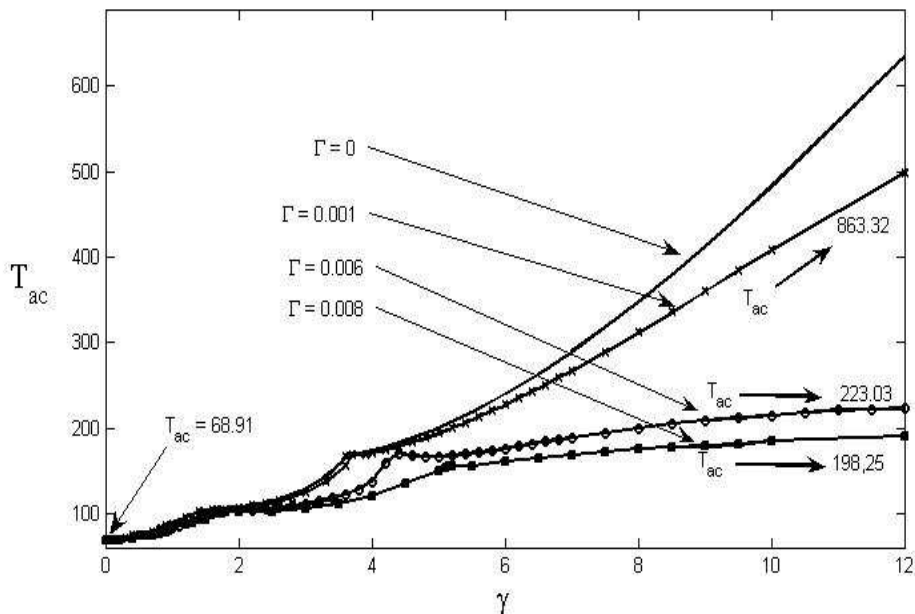


Fig. 3. Critical Taylor number versus the frequency number for different values of Deborah number Γ

The critical wave number versus γ is reported in Fig.3 for different values of Deborah number. The variation of q_c presents some discontinuities which occur at certain values of the parameter γ . The values of the parameter γ at which there are discontinuities, tend to shift toward to somewhat larger values.

In the low frequency limit, the critical wave number remains constant $q_c = 4$. This value corresponds to that of the classical Taylor-couette solution of a Newtonien fluid.

In the range of high frequency, the same behavior as that of the critical Taylor number occurs. For $\Gamma = 0$, the critical wave number increases versus the frequency number γ . However, we note that for $\Gamma = 0.001$ $\Gamma = 0.006$ and $\Gamma = 0.008$, the critical wave number becomes almost constant and takes respectevly the values depending only on Γ $q_c = 16.2$, $q_c = 7$ and $q_c = 6.5$. Finally, one can notice that the critical wave number decreases with increasing the Deborah number.

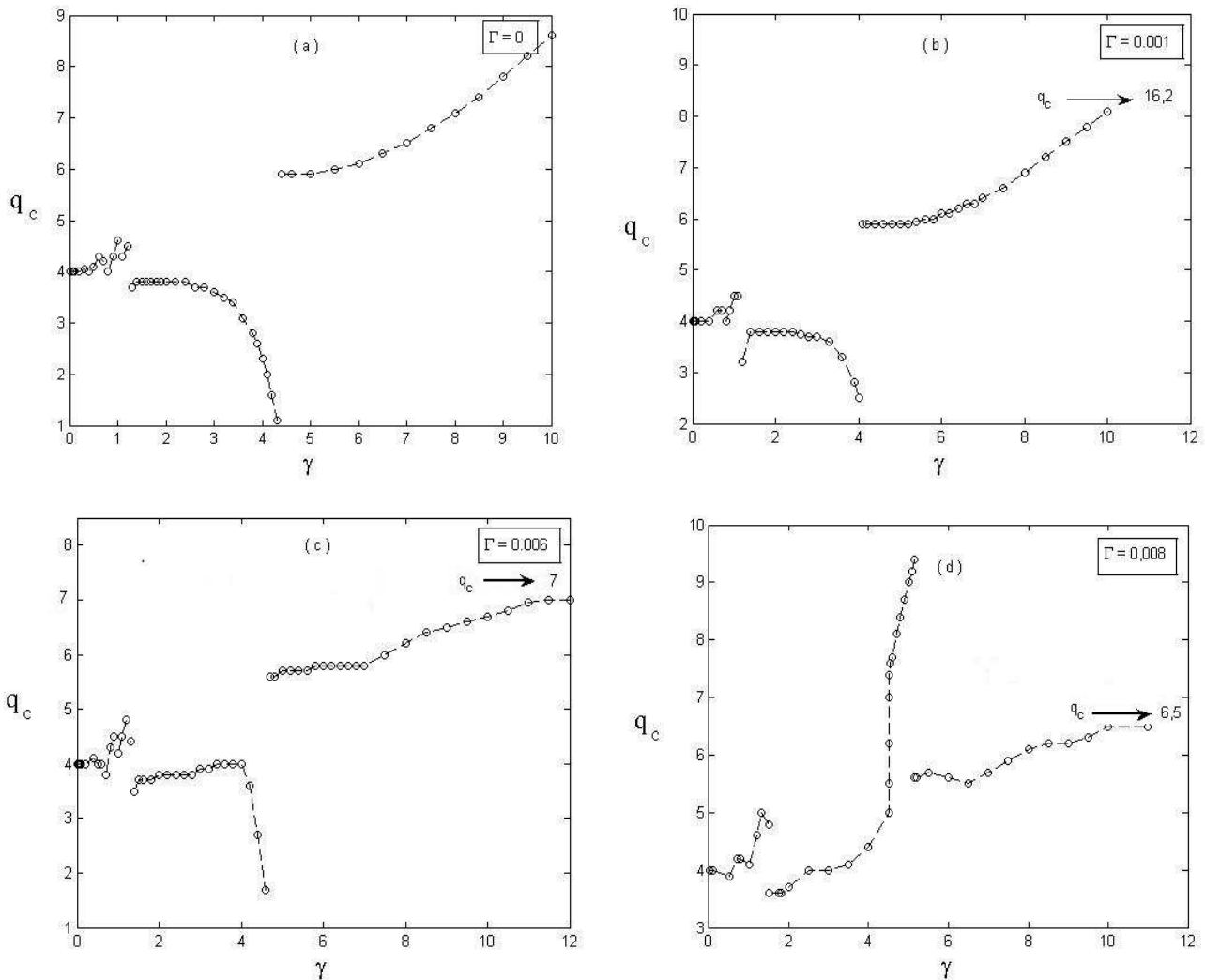


Fig. 4. Critical wave number versus the frequency number for different values of Deborah number Γ (a) : $\Gamma = 0$, (b) : $\Gamma = 0.001$, (c) : $\Gamma = 0.006$ (d) : $\Gamma = 0.008$

4 CONCLUSION

We have examined the linear stability of a pulsed flow of a viscoelastic fluid in the Taylor-Couette geometry when the outer and the inner cylinders are oscillating in out-of-phase with the same amplitude and frequency. We have focused on the effect of elasticity and frequency on the critical parameters, Taylor and wave numbers.

From a linear stability analysis, the numerical results have shown that at high frequencies, and in contrast to a Newtonian fluid, the critical Taylor and wave numbers are independent on the frequency number when Deborah number increases and the critical parameters tends to asymptotic values depending only on Deborah number. Furthermore, we have shown that

elasticity has a strong destabilizing effect. In this case only the spring will contribute to the total behavior in this frequency range. Decreasing the frequency number to intermediate frequency, the overall trend of the pulsed flow is toward more destabilization and the effect of elasticity is always destabilizing.

In the low frequency limit, the Maxwell fluid behaves as a Newtonian one and the critical Taylor number is given by $T_{ac} = 68.91$ which correspond to the unmodulated case. In this situation, the spring connected in series with a dashpot could be removed from the rheological model and only the dashpot will contribute to the total behavior.

REFERENCES

- [1] R. F. Donnelly, "Experiments on the stability of viscous flow between rotating cylinders. III Enhancement of stability by modulation.," *Proc. R. Soc. London Ser. A* 281, 130 (1964).
- [2] R. Thompson, "Instabilities of some time-dependent flows," Ph. D. Thesis, Massachusetts institute of technology (1968).
- [3] P. Hall, "The stability of unsteady cylinder flows," *J. Fluid Mech.* 67, 29 (1975).
- [4] P. J. Riley and R. Laurence, "Linear stability of modulated circular flow," *J. Fluid Mech.* 75, 625 (1976).
- [5] S. Carmi and J. I. Tustaniwskyi, "Stability of modulated finite-gap cylindrical Couette flow: linear theory," *J. Fluid Mech.* 108, 19 (1981).
- [6] T. J. Walsh and R. J. Donnelly, "Taylor-Couette Flow with Periodically Co-rotated and Counter-rotated Cylinders," *Phys. Rev. Lett.* 60, 700 (1988).
- [7] H. Kuhlmann, D. Roth and M. L\u00fcddeke, "Taylor vortices flow under harmonic modulation of the driving force," *Phys. Rev. A* 39, 745 (1989).
- [8] C.F. Barenghi and C. A. Jones, "Modulated Taylor-Couette flow," *J. Fluid Mech.* 208, 127 (1989).
- [9] C.M. Gassa Feugaing, O. Crumeyrolle, K.-S. Yang, I. Mutabazi, "Destabilization of the Taylor Couette flow of the inner cylinder rotation," *European Journal of Mechanics B/Fluids*, 44, 82-87, (2014).
- [10] A. Aouidef, C. Normand, A. Stegner and J. E. Wesfreid, "Centrifugal instability of pulsed flow," *Phys. Fluids*. 11, 3665 (1994).
- [11] A. Aouidef and C. Normand, "Instability of pulsed flow in Taylor-Couette geometry," *C. R. Acad. Sci. II B* 322, 545 (1996).
- [12] S. G. K. Tennakoon, D. Andreck, A. Aouidef, and C. Normand, "Pulsed flow between concentric rotating cylinders," *Eur. J. Mech., B/Fluids*, 16, No. 2 (1997).
- [13] E. Guyon, J. P. Hulin and L. Petit, *Hydrodynamique Physique*, EDP Sciences -CNRS Editions, 2001.
- [14] Platten J. K. and Legros J. C., "Convection in liquids", Springer-Verlag, Heidelberg, NewYork, (1984).